THE AMERICAN SOCIETY OF MECHANICAL ENGINEERS
345 E. 47 St., New York, N.Y. 10017





89-GT-1

# Experiments with a Low Specific Speed Partial Emission Centrifugal Compressor

**COLIN RODGERS**
Sundstrand Turbomach
San Diego, CA



## ABSTRACT

This paper describes experiments that were conducted several years ago on a single-stage open face centrifugal partial emission compressor with a non-dimensional specific speed of 0.15 (19.3 dimensional). The purpose of the experiments was to experimentally evaluate the partial emission compressor as a possible candidate for a high speed low flow natural gas fuel pump, the alternative to which was a larger heavier reciprocating compressor.

A review and re-analysis of the test data were conducted. The used updated compressor data reduction performance procedures and flow models to redefine the experimental compressor as a reference case in the low specific speed range of single-stage centrifugal compressors.

Normalized performance characteristics are presented for the experimental compressor in terms of efficiencies, diffuser recovery, and head coefficients versus diffuser relative flow parameter, or choke margin. Peak efficiency obtained at a De Laval number of 1.16, and nondimensional specific speed of 0.15, was 34.5%.

Stage performance is found to be dominated by diffuser geometry and choke margin, plus windage losses.

## NOMENCLATURE

| | |
|---|---|
| A | Throat Area |
| b | Axial Width |
| C | Absolute Velocity |
| $C_f$ | Friction Coefficient |
| $C_p$ | Static Pressure Recovery |
| D | Diameter |
| g | Gravitational Constant |
| H | Head |
| $M_u$ | De Laval Number |
| N | Rotational Speed |
| $N_s$ | Specific Speed (Dimensionless) |
| P | Total Pressure |
| p | Static Pressure |
| q | Work Factor |
| R | Radius - Gas Constant |
| RWD | Relative Flow Parameter |
| Re | Reynolds Number |
| S | Tip Gap |
| U | Tangential Velocity |
| W | Flow |
| $\Delta$ | Difference |
| $\eta$ | Adiabatic Efficiency |
| $\omega$ | Angular Velocity |
| $\Theta$ | Standard Temperature Correction |
| $\rho$ | Density |
| $\delta$ | Standard Pressure Correction |
| $\nu$ | Kinematic Viscosity |
| $\gamma$ | Specific Heat Ratio |

### Subscripts

| | |
|---|---|
| 1 | Impeller Inlet |
| 2 | Impeller Tip |
| 3 | Diffuser Throat |
| 4 | Diffuser Exit |
| m | Meridional |
| ad | Adiabatic |
| Crit | Critical |
| RDF | Recirculation and Disc Friction |
| ov | Overall |
| th | Theoretical |

Presented at the Gas Turbine and Aeroengine Congress and Exposition—June 4-8, 1989—Toronto, Ontario, Canada
This paper has been accepted for publication in the Transactions of the ASME
Discussion of it will be accepted at ASME Headquarters until September 30, 1989

## INTRODUCTION

The wide diversity of applications for centrifugal compressors and pumps cover impeller designs ranging from non-dimensional inlet specific speeds as low as 0.3, to as high as 1.5 where:

$$N_s = \omega\left(\frac{W}{\rho_1}\right)^{0.5}(gH_{ad})^{-0.75}$$

Although low specific speed stages are inherently inefficient, they may be used as exit stages in multi-stage industrial compressors, gas turbine fuel pumps, and in special low flow circumstances where optimal choice of rotational speed is not possible.

The classic specific speed charts of Balje (1) indicate that choices for very low specific non-reciprocating compressors are of the following type:

- Partial Emission
- Drag
- Pitot Pump
- Multiple Lobe (Vane Motor)

Additionally, Wedge type impellers are recommended by Rusak (2) for low specific speed centrifugal compressor applications.

Extensive development of partial emission pumps for rocket motor applications was described by Barske (3) who found that some aspects of common centrifugal pump design such as optimum blade geometries were apparently less important in very low flow regimes. The major advantage of dynamic (non-reciprocating) compressors is compactness inherent with high speed operation, and in weight/volume constrained intermittent duty applications where compressor efficiency may be compromised in favor of compactness.

The design requirements for special propulsion systems faced by Barske suggested the employment of some kind of positive displacement pump or a multi-stage centrifugal pump. A preliminary design assessment, however, showed that such approaches were too heavy and complicated.

Following the innovative work of Barske, the author in 1962 became associated within the development of a partial emission natural gas compressor to be directly driven at 35,000 rpm by a gas turbine as its own fuel pump.

The partial emission centrifugal compressor, or pump, is categorized by a simple paddle rotor or impeller, enclosed in a tight fitting scroll usually with a single port diffuser capturing the impeller exit flow over a small arc of its periphery.

This paper describes experiments that were conducted on a 10.38 inch (263 mm) diameter partial emission gas compressor and identifies design performance parameters which basically influence the pressure, flow and efficiency characteristics of such turbomachines.

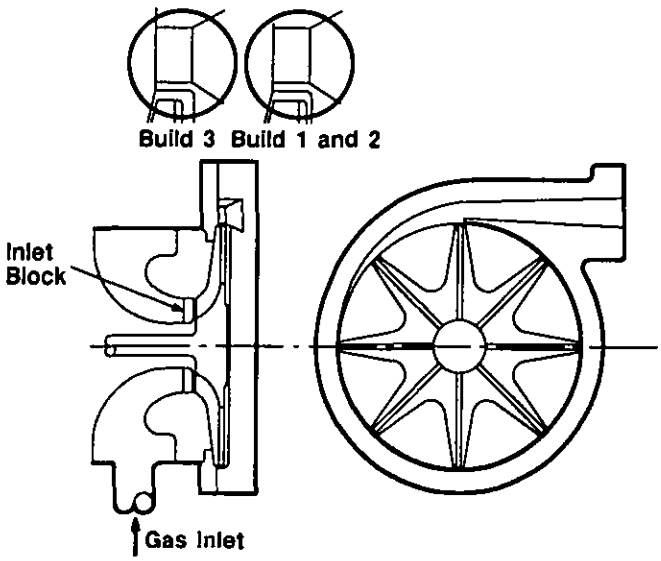


*Figure 1. Partial Emission Compressor*

## COMPRESSOR DESIGN FEATURES

Adhering to the design recommendations of Barske, the partial emission gas compressor shown in Figure 1 was designed and fabricated for an exploratory compressor test program.

The gas compressor was designed for the following conditions:

| | |
|---|---|
| Natural Gas Flow | 320 pph (121 kg/hr) |
| Pressure Ratio | 2.3 |
| Rotational Speed | 35,000 rpm |
| Gas Specific Heat Ratio, $\gamma$ | 1.27 |
| Gas Constant, R | 86 |
| Inlet Pressure | 15.0 psia (1.02 bar) |
| Inlet Temperature | 540°R (300°K) |
| De Laval Number, $U\sqrt{(g\gamma RT_1)}0.5$ | 1.25 |

The open face eight radially bladed impeller and single channel discharge diffuser are shown in Figure 2. Geometric features of the impeller and diffuser are listed in Figure 3. The impeller inlet design was constrained by the requirement to adapt an existing compressor rig, shaft, and bearing capsule assembly. The design diffuser had an area ratio of 6.25 combined with a length-to-inlet width ratio of 15.0. The expected static pressure recovery coefficient was approximately 0.5 assuming an inlet blockage of .05.

## COMPRESSOR RIG AND INSTRUMENTATION

Figure 4 shows a photograph of the partial emission compressor installed in the test facility. The compressor was driven by a 200-hp electric dynamometer driving through a step-up gearbox with a speed increasing ratio of 23.8. The dynamometer was trunnion mounted, and provided input torque data to determine compressor power. This is of particular importance in low specific speed compressor performance assessment where casing heat losses can represent a significant fraction of the enthalpy rise.

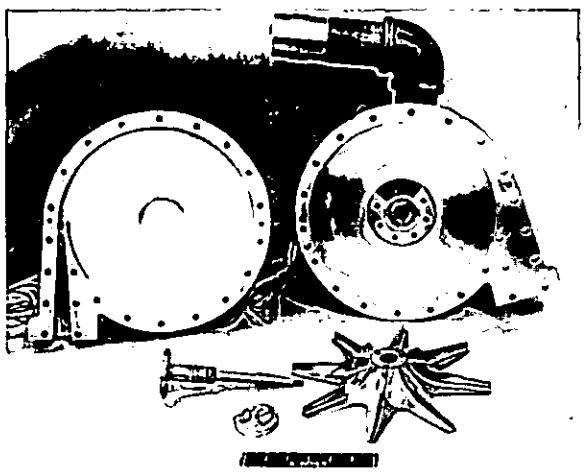

Figure 2. Partial Emission Compressor Components

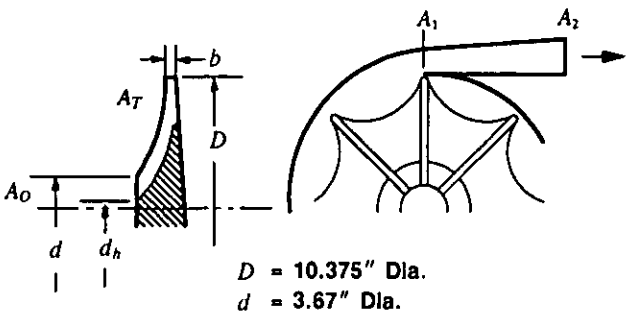


$D$ = 10.375" Dia.
$d$ = 3.67" Dia.
$d_h$ = 2.05" Dia.

| | Build Number | | |
|---|---|---|---|
| | 1 | 2 | 3 |
| D/DTH | 19.5 | 19.5 | 20.3 |
| D/d | 2.74 | 2.74 | 2.74 |
| b/D | 0.0472 | 0.0472 | 0.289 |
| $A_O$ (sq. in.) | 7.803 | 1.951 | 1.951 |
| $A_T$ (sq. in.) | 15.971 | 16.971 | 9.778 |
| $A_T/A_O$ | 2.05 | 8.19 | 6.01 |
| $A_1$ (sq. in) | 0.220 | 0.220 | 0.204 |
| $A_2$ (sq. in) | 1.375 | 1.375 | 1.360 |
| $A_2/A_1$ | 6.25 | 6.25 | 6.67 |

Figure 3. Compressor Geometric Features

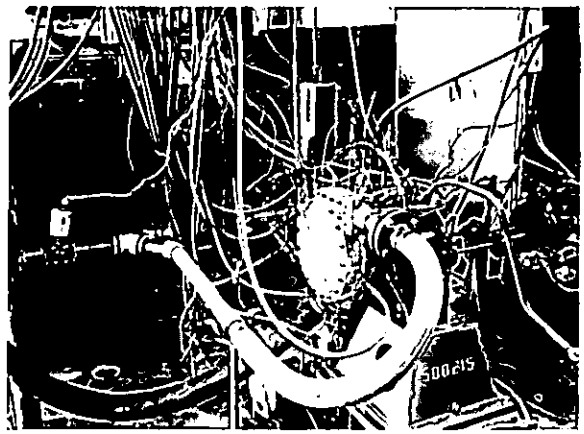

Figure 4. Test Facility

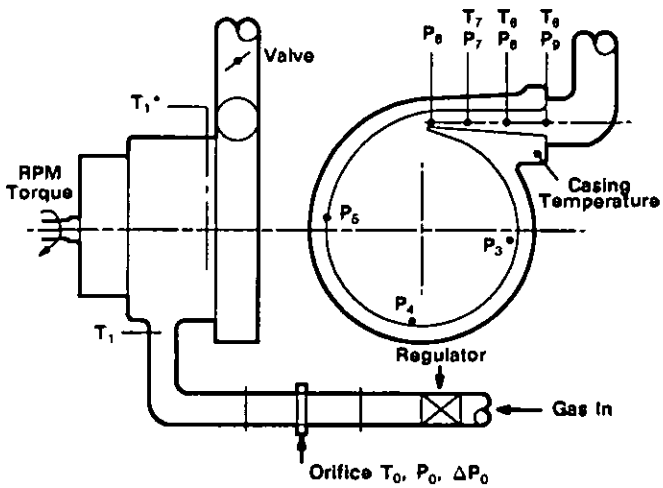


Static Pressures, Total Temperatures

| Data | Description | No. |
|---|---|---|
| $T_0$ | Orifice Temperature | 1 |
| $P_0$ | Orifice Pressure | 1 |
| $\Delta P_0$ | Orifice Differential | 1 |
| $T_1$ | Inlet Temperature | 1 |
| $T_1$' | Rotor Inlet Temperature | 3 |
| $P_3$, $P_4$, $P_5$ | Rotor Tip Pressure | 3 |
| $P_6$, $P_7$, $P_8$, $P_9$ | Diffuser Pressures | 4 |
| $T_7$, $T_8$, $T_9$ | Diffuser Temperatures | 3 |

Figure 5. Test Instrumentation

Natural gas was introduced from a regulator, controlled at the operating panel through a standard ASME orifice run to the compressor inlet casing. Compressor flow was controlled by a butterfly valve located in the discharge pipe. The natural gas used during testing was piped to a burner located on the test facility roof.

The compressor casing and volute were fabricated from aluminum and testing was therefore limited to a maximum casing temperature of 910°F (506°K). Casing insulation was installed for test calibrations.

Compressor test instrumentation is shown in Figure 5. A 0.6 inch diameter (15.2mm) orifice was used in a 2.375 inch diameter (60.5 mm) pipe for flow measurement.

## CALCULATION PROCEDURE

The stage static pressure rise, total temperature rise, and adiabatic efficiency were computed from the measured pressures and temperatures using a constant average specific heat ratio of 1.27.

Impeller and diffuser performances were calculated from the measured overall temperature rise and static pressures at the impeller tip, diffuser throat, and diffuser exit, using standard data reduction codes with Wiesner slip factor as input to assess average (mixed out) vector triangles at the three stations. This technique, although not an absolute measurement, has provided a convenient yardstick for impeller efficiency assessment.

An intrinsic weakness of the technique, however, is the inability to rate the quality of the impeller exit flow distribution and wake mixing effects on the downstream diffusion system. It has been determined that impeller performance calculated in this manner does not always exhibit acceptable repeatability when the downstream diffusion process is changed.

Representation of the impeller tip flow conditions by either blockage, jet and wake momentum deficiency, or profile corrections is a debatable subject in both radial and axial compressor design. It becomes a matter of the taste and experience of the individual designers.

Initial analysis using the mixed-out model revealed stagnation pressure inconsistencies between vector conditions at the impeller tip and diffuser throat. A meaningful stagnation pressure balance could only be satisfied (with slip as input) using only 2.5% of the impeller tip flow area as an active arc of emission. This intuitively can be visualized from Figure 1 as a plausible flow model, where large amounts of internal recirculation occur within the impeller, with only the small diffuser throat area available through which the flow can escape.

An uncertainty error computation was conducted to determine the approximate limits of the instrumentation used to evaluate overall compressor efficiency. An approximation of error, assuming maximum error in the instrumentation system, indicated an uncertainty in computation of efficiency of $\pm$ 0.8 percentage points from a design efficiency of 40.0 percent. Flow measurement error varied from $\pm$ 1% near rated flow to as high as $\pm$ 6% at lower flows.

The calculations did not take into account any errors caused by actual installation of sensors in the system. The system was calibrated prior to test, and all calibration corrections were applied. The system was operated at a stable ambient temperature very near the design conditions when calibrated. At 100 percent design speed, variation in upstream pipe inlet and exit discharge temperatures were 2.0 and 4.0°F, respectively.

Test data analysis was originally completed using desk top calculators. For re-examination purposes all data were recompiled and computed with current compressor rig performance analysis codes.

Due to the dominance of partial emission compressor performance by the single exit diffuser, it was elected to present test data using the following compressor performance parameters:

Relative Flow Parameter (or Choke Margin)
$$RWD = \frac{\left(\frac{W\sqrt{T}}{AP}\right)_3}{\left(\frac{W\sqrt{T}}{AP}\right)_{3critical}}$$

Overall Efficiency
$$Based\ on\ \frac{p_4}{p_1}$$

Impeller Efficiency
$$Based\ on\ \frac{P_2}{p_1}$$

Diffuser Static Pressure Recovery
$$C_{p\ 3\text{-}4} = \frac{p_4 - p_3}{P_2 - p_2}$$

Work Factor
$$q = \frac{gJC_p\Delta T}{U_2^2}$$

Windage and Recirculation
$$q_{RDF} = \frac{q - gJC_p\Delta Tth}{U_2^2}$$

## TEST RESULTS

Compressor testing encompassed three different compressor configurations identified in Table 1. Test results for each of the three builds are discussed as follows.

*Table 1. Test Configurations Impeller Tip Diameter = 10.375 In*

| | | BUILD NUMBER | | |
|---|---|---|---|---|
| | | 1 | 2 | 3 |
| Impeller Inlet Area | sq in | 7.8 | 1.95 | 1.95 |
| Impeller Exit Width | in | 0.49 | 0.49 | 0.30 |
| Diffuser Throat Area | sq in | 0.22 | 0.22 | 0.204 |
| Diffuser Exit Area | sq in | 1.38 | 1.38 | 1.36 |

*Build 1*

A complete performance characterization was acquired for the initial configuration covering 60, 80, 90, and 100% corrected speed from choke to the minimum flow constrained by either the maximum casing temperature limit, or one inch Hg differential pressure across the orifice plate. No surging characteristics were exhibited by the compressor. Inlet temperatures immediately adjacent to the impeller in the recirculation zone exhibited an increasing spread as flow was reduced. At minimum flow and rated speed the temperature rise above the upstream inlet temperature was of the order 80°F (27°C).

The performance characteristics for Build are normalized on Figure 6 in terms of the selected performance parameters vs. the relative flow parameter (choke margin), RWD. Although some scatter is apparent, a near unique stage characteristic results. A peak overall adiabatic efficiency of 31.8% was

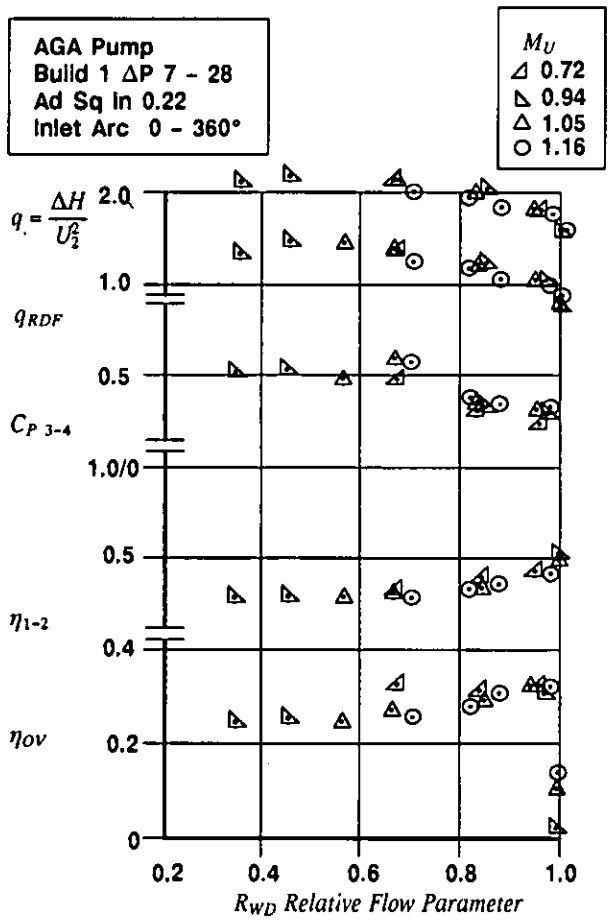


*Figure 6. Build 1 Performance Characteristics*

obtained at a rated speed with relative flow parameter, RWD of 0.97. Corresponding overall pressure ratio was 2.38, close to the design goal of 2.3.

It was apparent that-from both examination of the windage and recirculation factor $q_{RDF}$ and inlet temperature recirculating measurements, that the major loss was stemming from impeller windage effects. Diffuser static pressure recovery of 0.4 to 0.5 was close to expected limits for an area ratio of 6.25 and length to width ratio of 15.0 (covered passage/throat).

Examination of the compressor efficiency computed from work and temperature rise showed that at and near choke the two methods agreed within the limits of the test accuracy, but that at the minimum flow, efficiency computed from work was subject to increased scatter as a consequence of flow measurement inaccuracies towards shut off.

Impeller tip static pressure ratios at each of the test speeds and near peak overall efficiency are shown in Figure 7. A large static pressure rise occurs towards the diffuser throat as a consequence of diffusion on the pre-throat region. Some possible acceleration of the flow in the confined interspace towards the pre-throat is indicated. Impeller efficiency was computed using the arithmetic average tip static pressures ($p_3$, $p_4$, $p_5$).

The large windage and recirculation effects encountered on the first build suggested the use of an inlet block similar to that tried by Van Le (4) could diminish recirculation losses. An inlet blockage plate was therefore fabricated as shown in Figure 2 blocking off 75% of the impeller inlet eye annulus. Evidence of flow recirculation back to the impeller inlet is illustrated by the flow traces in Figure 8.

*Build 2*

The inlet block was installed initially to block off the first 270 deg arc from top dead center (TDC). A complete performance map was re-run and the test results are shown in Figure 9. Windage and recirculation losses were reduced 25% and maximum recorded overall efficiency increased to 34.5%. Commensurate with the reduction in windage and recirculation losses, the overall work factor also decreased with a corresponding reduction in pressure ratio from 2.38 to 2.31 as listed in Table 2. The performance improvement further suggested extending test calibrations to include the effect of blockage circumferential orientation in relation to the throat tongue or TDC. Accordingly additional testing was conducted on Build 2 at rated speed only with various blockage orientations, and results are depicted in Figure 10. These data indicate no distinct optimum orientation of the blockage plate. Some minor shifts in impeller tip static pressure distributions were noticed, dependent upon blockage plate orientation.

*Table 2. Test Results 100% Corrected Speed*

| | | BUILD NUMBER | | |
|---|---|---|---|---|
| | | *1* | *2* | *3* |
| Data Point Number | | 24 | 44 | 79 |
| Overall Efficiency | % | 31.4 | 34.5 | 32.2 |
| Relative Flow Parameter | RWD | 0.97 | 0.99 | 0.98 |
| Dimensionless Specific Speed | | 0.145 | 0.156 | 0.161 |
| Pressure Ratio | | 2.38 | 2.31 | 2.10 |
| Inlet Corrected Flow | pps | 0.123 | 0.135 | 0.118 |
| Work Factor | | 1.75 | 1.54 | 1.43 |
| Windage & Recirculation Factor | $q_{RDF}$ | .974 | 0.76 | 0.66 |
| Impeller Efficiency | 1-2 % | 39.0 | 45.3 | 45.9 |
| Efficiency | 1-3 % | 42.0 | 50.7 | 47.0 |
| Diffuser Static Pressure Recovery | $C_{P\ 3-4}$ | 0.34 | 0.29 | 0.21 |
| Compressor Horsepower | | 34.5 | 33.7 | 28.7 |
| Windage Recirculation Horsepower | | 19.2 | 16.6 | 13.1 |

*Build 3*

In an attempt to achieve the design goal efficiency of 40% it was postulated that windage recirculation losses could be reduced further by increasing the radial velocity component at the impeller tip. Accordingly the impeller tip width was reduced approximately one-third and restricted to the diffuser as shown in Figure 1. This restacking caused a reduction in

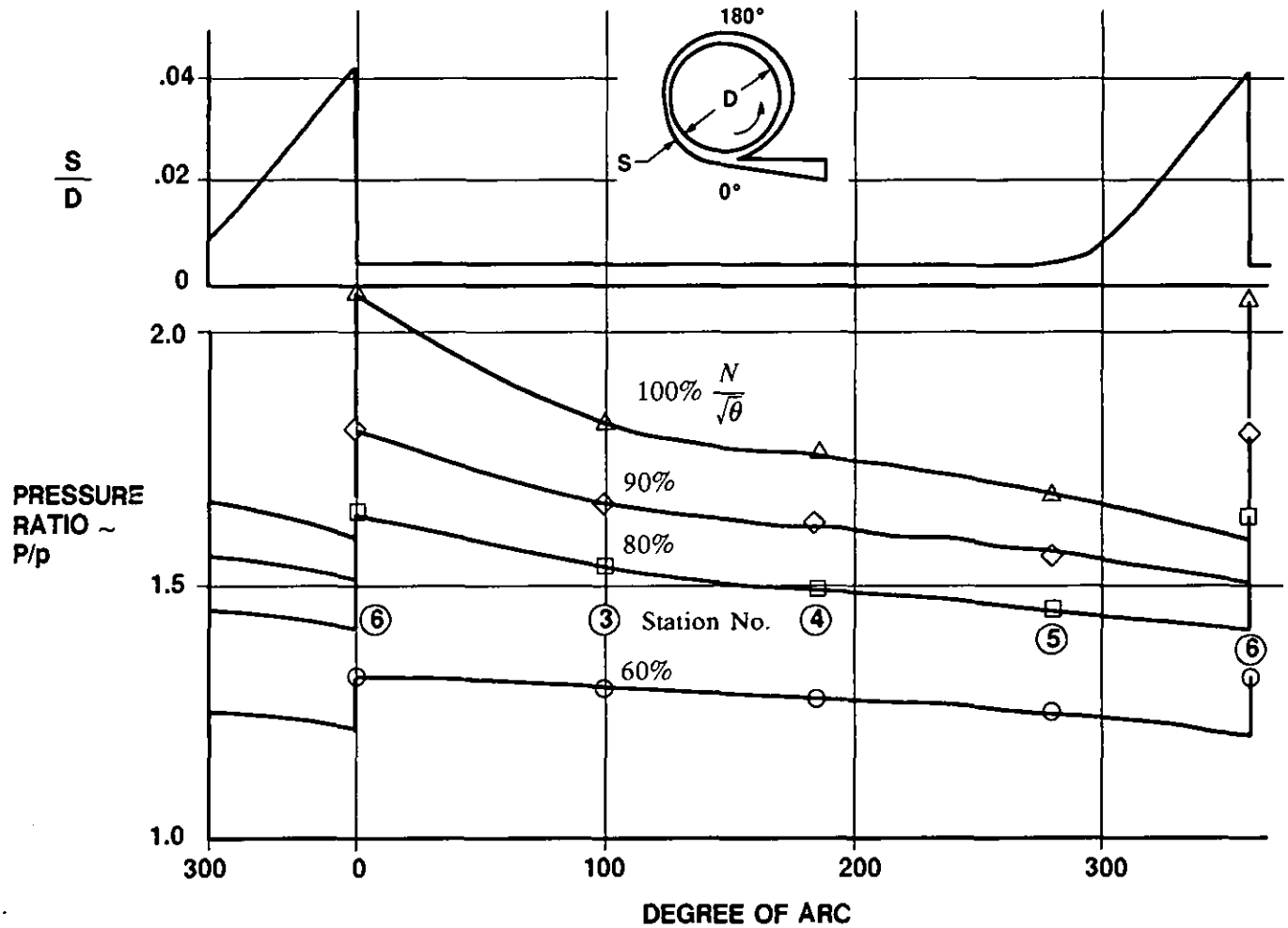


*Figure 7. Impeller Tip Static Pressure Distribution at Peak Efficiency*

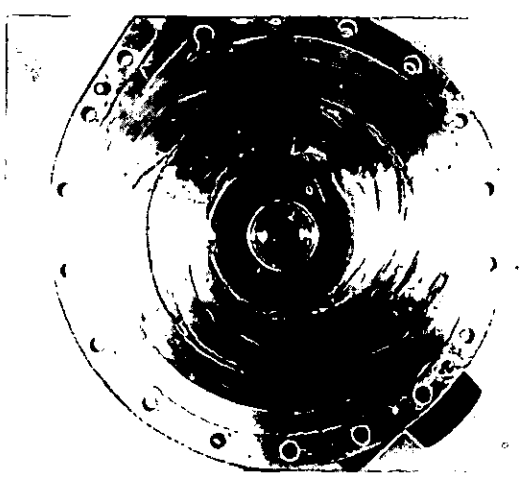

*Figure 8. Recirculation Flow Traces*

diffuser throat area of 7% in addition to passage width expansion of 27% between the impeller tip and throat.

Test data for Build 3 is shown in Figure 11 and indicates that although windage and recirculation losses were further slightly reduced, the diffuser static pressure recovery coefficient fell to 0.2.

Comparative performances for all three builds at rated speed and near peak efficiency are listed in Table 2.

## DISCUSSION

The test data obtained from the three compressor builds can be summarized in the following finding:

- Windage and recirculation losses are large, but do contribute to the stage head rise capability.
- Diffuser performance corroborates with expected levels of static pressure recovery (5) providing the interspace transition is smooth.
- No surge instabilities of the partial emission compressor were observed for the test range of pressure ratios.
- Peak efficiency occurred near diffuser choke and attained a test maximum level of 34.5%.

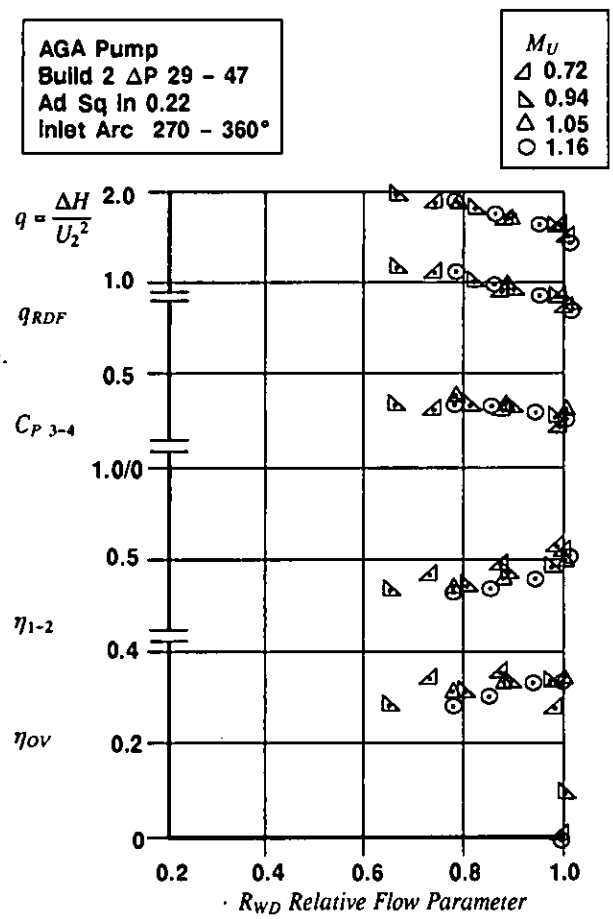


Figure 9. Build 2 Test Results

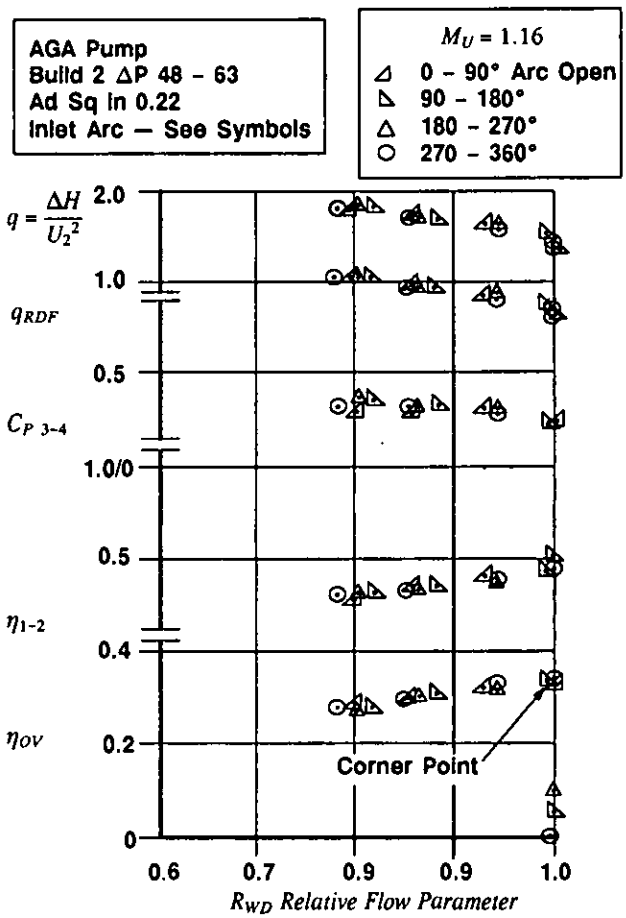


Figure 10. Build 2 Test Results With Various Blockage Orientations

- Diffuser performance decreased insignificantly with a 27% increase in passage width between the impeller tip and throat.

A conventional compressor map representation of Build 2 test performance is shown in Figure 12 in terms of inlet corrected airflow, pressure ratio, and efficiency, with corrected speed as a parameter. Note that the low flow end points are not surge points but a low flow limit constrained by casing temperature limitations.

Balje (1, Figure 6.81) indicates that slightly higher peak efficiency islands of 40% are attainable and corroborates that recirculation losses are dominant. An equivalent disc friction coefficient and Reynolds number were computed from the windage and recirculation losses defined by:

$$Cf = \frac{g_{Torque}}{\varrho\omega^2 R^5} \qquad \mathrm{Re} = \frac{\omega R^2}{\upsilon_{1-2}}$$

Test friction coefficients are plotted on Figure 13 and show decreasing values for successive builds 1, 2 and 3. Superimposed in Figure 13 are the data from Ref. 6 for an eight bladed rotor in an enclosed vessel with a hub/tip ratio less than 0.6 and $b/D_2$ ratio of .047. Comparison of the data indicates the major loss source is indeed windage as would be expected as the compressor specific speed approaches zero. Wider tip widths and full inlet admission appear to increase recirculation (or pumping) losses.

A quick evaluation of the corner-point peak efficiency (near choke) performance of a partial emission compressor can be assessed using the procedure of Appendix 1. Either the flow can be input to determine the required diffuser throat area or alternately the flow capability of a given geometry can be calculated using the throat area as input. The impeller efficiency model assumes efficiency increases with increasing speed according to the trends of Refs. 3 and 7.

## CONCLUSION

A major intent of reviewing and re-analyzing the experimental single-stage partial emission compressor was to establish it as a reference case in low specific speed centrifugal compressor turbomachinery technology. It is fundamentally difficult to obtain good efficiencies in such applications intrinsically due to large windage and recirculation losses. Examination of the stage test data indeed confirms that these losses can equal the theoretical head input. Although such losses detract from the efficiency potential of partial emission compressors, they do provide useful head.

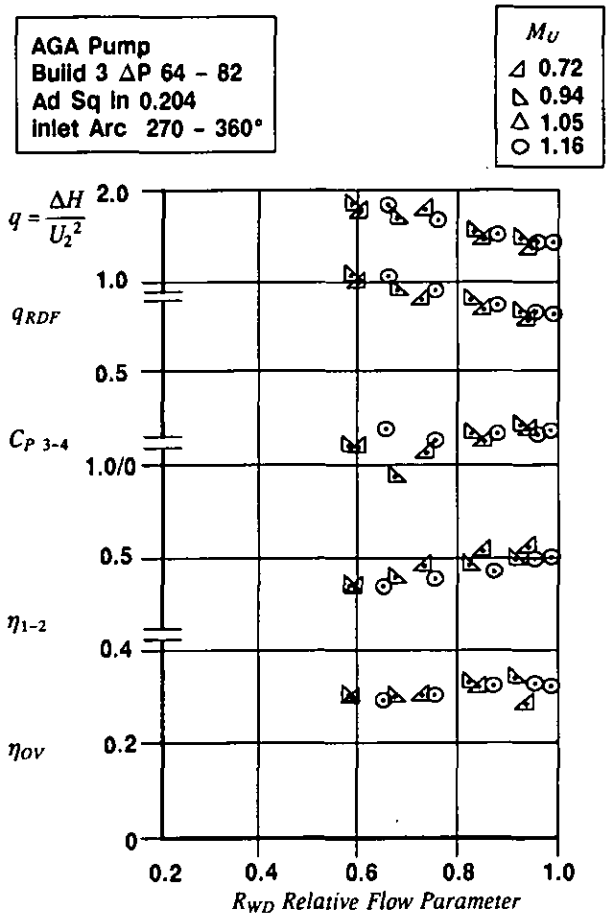


*Figure 11. Build 3 Test Results*

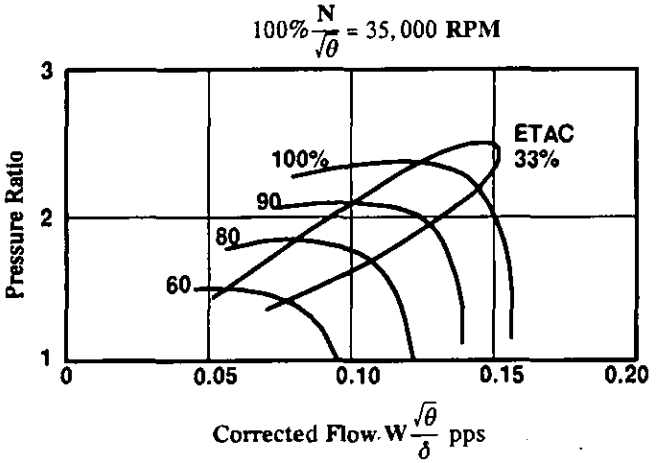


*Figure 12. Partial Emission Compressor Map, Build 2*

Windage and recirculation losses were reduced 25% by blocking off three quarters of the impeller inlet annulus. This combined with the same effective blockage at the impeller tip, left one quarter of the impeller flow-path actively scavenging and exhausting. Tests with various angular orientations of the inlet blockage plate to the diffuser throat tongue, revealed no distinct optimum location.

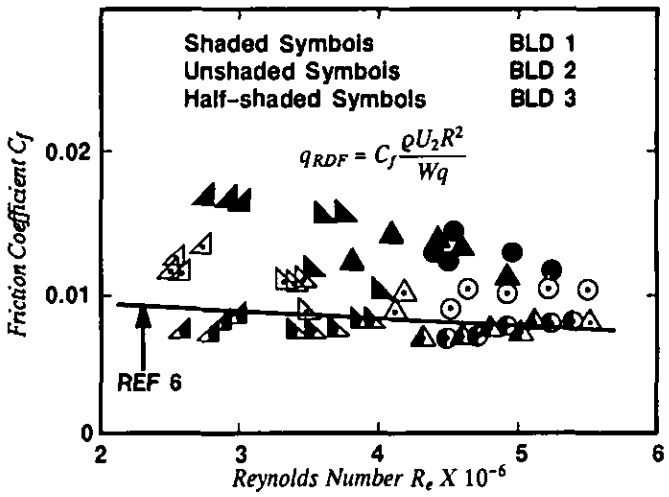


*Figure 13. Windage and Recirculation Losses*

Windage and recirculation losses were further reduced 14% by decreasing the impeller tip width one third. This however resulted in a passage expansion between the impeller tip and diffuser throat, adversely influencing the diffuser performance and reducing overall stage efficiency by up to 3% points.

The diffuser dominated the whole stage matching, performing close to expectations in terms of static pressure recovery. Stage performance was normalized on the basis of diffuser relative flow parameter (RWD) or choke margin, and as such revealed a near unique characteristic for all test speeds. Peak stage efficiency occurred adjacent (within 10%) to diffuser choke and attained a maximum value of 34.5% at a non-dimensional specific speed of 0.15.

Ref. 3 shows that efficiencies as high as 57% can be obtained at higher specific speeds in the 0.3 range with pumps, and probably more pump performance data may be found in open literature. Commercial partial emission compressors are produced under the trade name of Sundyne (see Ref. 7 and Figure 14), and are capable of peak adiabatic efficiencies in the 41% region at an optimum specific speed of 0.3 with Mach numbers Mu of 1.15.

A major disadvantage of partial emission compressors is the high heat generated by the windage and recirculation losses which can severely limit their application.

## LIST OF REFERENCES


1. Balje, O.E., "Turbomachines". Wiley Interscience.
2. Rusak, V., 1982, "Development and Performance of the Wedge-Type Low Specific Speed Compressor Wheel", ASME 82-GT-214.
3. Barske, V.M., 1959, "Development of Some Unconventional Centrifugal Pumps", Inst. of Mechanical Engineers Vol. 21
4. Van Le, N., 1961, "Partial Flow Centrifugal Compressors", ASME 61-WA-135.

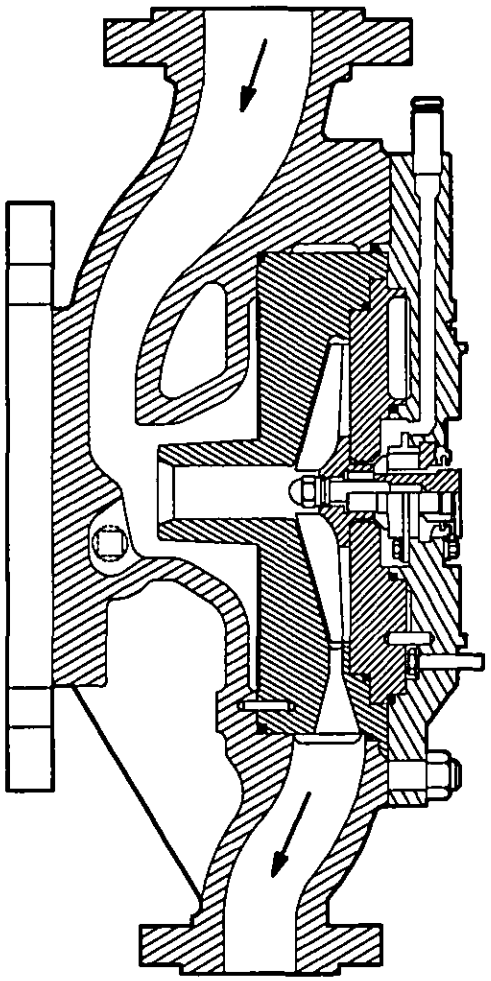

*Figure 14. Commercial Partial Emission Compressor*


5. Reneau, L.R., Johnston, J.P., Kline, S.J., 1967, "Performance and Design of Straight Two Dimensional Diffusers". ASME Trans JBE Vol. 89D.

6. Furuya, Y., Watabe, K., 1964, "On the Racing Power of Impellers". Bulletin of JSME, Vol. 7 No. 36

7. Sundstrand Fluid Handing, 1986, "Sundyne Compressor Fuel Selection Procedure". P.O. Box FH, Avrada, Colorado 80004.

## APPENDIX. CORNER POINT MODEL

Input Inlet pressure, temperature, flow P, T, W
Impeller Tip Speed $U_2$
Work Factor ($q_{slip}$ + $q_{RDF}$)
Diffuser Static Pressure Recovery $C_{P\ 3-4}$

Impeller Pressure Ratio

$$\frac{P_2}{P_1} = \left(1 + \eta_{1-2}\frac{q}{gJC_p}\left(\frac{U_2}{\sqrt{T_1}}\right)^2\right)^{\frac{\gamma}{\gamma-1}} \tag{1}$$

Initially assume $\eta_{1-2} = 0.45$

Assume no core stagnation loss between stations 2 and 3

$$\frac{P_3}{P_1} = \frac{P_2}{P_1} \qquad \frac{T_3}{T_1} = \frac{T_2}{T_1} = \left(\frac{P_2}{P_1}\right)^{\frac{\gamma-1}{\gamma}} \tag{2}$$

Assume peak corner point pressure ratio of RWD = 0.975

($M_3 \simeq .85$), then diffuser throat area is given by:

$$A_3 = \frac{1}{RWD}\ \frac{W\sqrt{T_1}}{P_1}\sqrt{\frac{T_3}{T_1}}\ \frac{P_1}{P_3}\ \frac{1}{\left(\frac{W\sqrt{T_3}}{(P_3A_3)}\right)_{CRIT}} \tag{3}$$

$$\left(\frac{P}{p}\right)_3 = \left(1 + \frac{\gamma-1}{2}\ M_3^2\right)^{\frac{\gamma}{\gamma-1}} \tag{4}$$

Diffuser Geometry

Select $A_4$, $L_{3-4}$ and determine $C_{P3-4}$ from Ref. 5.

$$P_4 = \left(\frac{p}{P}\right)_3 + C_{P3-4}\left(1 - \left(\frac{p}{P}\right)_3\right) \tag{5}$$

$$\frac{P_4}{P_1} = \frac{P_3}{P_1}\ \frac{P_4}{P_2}$$

$$\text{Overall Efficiency}\quad \eta_{1-4} = \left[\frac{\left(\frac{P_4}{P_1}\right)^{\frac{\gamma-1}{\gamma}} - 1}{\left(\frac{P_3}{P_1}\right)^{\frac{\gamma-1}{\gamma}}}\right]\eta_{1-3} \tag{6}$$

$$\text{Specific Speed}\quad N_s = \omega\frac{\sqrt{\frac{W}{\varrho_1}}}{(gH_{ad})^{.75}} \tag{7}$$

$$\text{Check Impeller Efficiency}\quad \eta_{1-2} = 0.6\left|1 - \left(1 - \frac{N_s}{0.3}\right)^2\right|$$